A hydrogeological study of the Nhandugue River, Mozambique – A major groundwater recharge zone

Article *in* Physics and Chemistry of the Earth Parts A/B/C · December 2011

DOI: 10.1016/j.pce.2011.07.036

6 authors, including:

F. Chirindja
Eduardo Mondlane University
4 PUBLICATIONS **2** CITATIONS
SEE PROFILE

Torleif Dahlin
Lund University
179 PUBLICATIONS **3,370** CITATIONS
SEE PROFILE

Richard Owen
University of Zimbabwe
30 PUBLICATIONS **211** CITATIONS
SEE PROFILE

Franziska Steinbruch
Deutsche Gesellschaft für Internationale Zus…
23 PUBLICATIONS **58** CITATIONS
SEE PROFILE

Physics and Chemistry of the Earth 36 (2011) 789–797

Contents lists available at SciVerse ScienceDirect

Physics and Chemistry of the Earth

journal homepage: www.elsevier.com/locate/pce

A hydrogeological study of the Nhandugue River, Mozambique – A major groundwater recharge zone

K. Arvidsson [a], L. Stenberg [a], F. Chirindja [b], T. Dahlin [c,*], R. Owen [d], F. Steinbruch [e]

[a] Dept. of Earth and Ecosystem Sciences, Lund University, Sölvegatan 12, SE-22362 Lund, Sweden
[b] Geology Dept., Eduardo Mondlane University, Maputo, Mozambique
[c] Engineering Geology, Lund University, Box 118, SE-22100 Lund, Sweden
[d] Geology Dept., University of Zimbabwe, Harare, Zimbabwe
[e] Scientific Services, Gorongosa National Park, Sofala, Mozambique

ARTICLE INFO

Article history:
Available online 12 August 2011

Keywords:
Gorongosa National Park
Groundwater recharge zone
Hydrogeology
Resistivity
Urema Rift

ABSTRACT

The Nhandugue River flows over the western margin of the Urema Rift, the southernmost extension of the East African Rift System, and marks the north-western border of Gorongosa National Park, Mozambique. It constitutes one of the major indispensable water resources for the ecosystem that the park protects. Our study focused on the hydrogeological conditions at the western rift margin by resistivity measurements, soil sampling and discharge measurements. The resistivity results suggest that the area is heavily faulted and constitutes a major groundwater recharge zone. East of the rift margin the resistivity indicate that solid gneiss is fractured and weathered, and is overlain by sandstone and alluvial sediments. The top 10–15 m of the alluvial sequence is interpreted as sand. The sand layer extends back to the rift margin thus also covering the gneiss. The sandstone outcrops a few kilometers from the rift margin and dips towards east/south-east. Further into the rift valley, the sand is underlain by lenses of silt and clay on top of sand mixed with finer matter. In the lower end of the investigated area the lenses of silt and clay appears as a more or less continuous layer between the two sand units. The topmost alluvial sand constitutes an unconfined aquifer under which the solid gneiss forms a hydraulic boundary and the fractured gneiss an unconfined aquifer. The sandstone is an unconfined aquifer in the west, becoming semi-confined down dip. The lenses of silt and clay forms an aquitard and the underlying sand mixed with finer matter a semi-confined aquifer. The surface runoff decreases downstream and it is therefore concluded that surface water infiltrates as recharge to the aquifers and moves as groundwater in an east/south-eastward direction.

1. Introduction

1.1. Location of the area

Gorongosa National Park (GNP) is situated at 19°S and 34°W, within the Sofala province in the central part of Mozambique (Fig. 1). The park is located within the southernmost extension of the East African Rift System (EARS), the Urema Rift, and covers an area of approximately 3770 km^2. The park protects a vast ecosystem of floodplains, grasslands and woodlands.

1.2. Geology and geomorphology

The rift valley floor constitutes the lowest part of the park and it is filled with mainly Quaternary alluvial sediments, in west resting on top the Sena Formation (Fig. 2; Lächelt, 2004). East of the rift margin the Sena Formation and also the Lupata Group are outcropping north respectively south of the Nhandugue River. The Sena Formation consists of massive conglomeratic arcosic sandstones and the Lupata Group comprises red conglomeratic sandstones and phonolitic lava (Tinley, 1977; Lächelt, 2004; National Directorate of Geology, 2006). In general coarse alluvial sediments, like gravel and sand, have formed alluvial fans on the sides while finer sediments have been deposited further out on the valley floor (Tinley, 1977; Chirindja and Hellman, 2009). Sets of NNE–SSW and NNW–SSE orientated faults and fracture zones on both sides of the Urema Rift (Tinley, 1977) are responsible for the system of half-grabens that constitute the 40 km wide rift valley. On the eastern side the valley is defined by the Cheringoma Platform and on the western side it is bounded by the Báruè Platform (Fig. 2). Rising west of the Báruè Platform is the Gorongosa Mountain.

1.3. Climate and drainage

For the function of the ecosystem water resources are indispensable. Several rivers are flowing into the park and merges in

* Corresponding author. Tel.: +46 46 222 96 58; fax: +46 46 222 91 27.
E-mail address: torleif.dahlin@tg.lth.se (T. Dahlin).

1474-7065/$ - see front matter © 2011 Elsevier Ltd. All rights reserved.
doi:10.1016/j.pce.2011.07.036

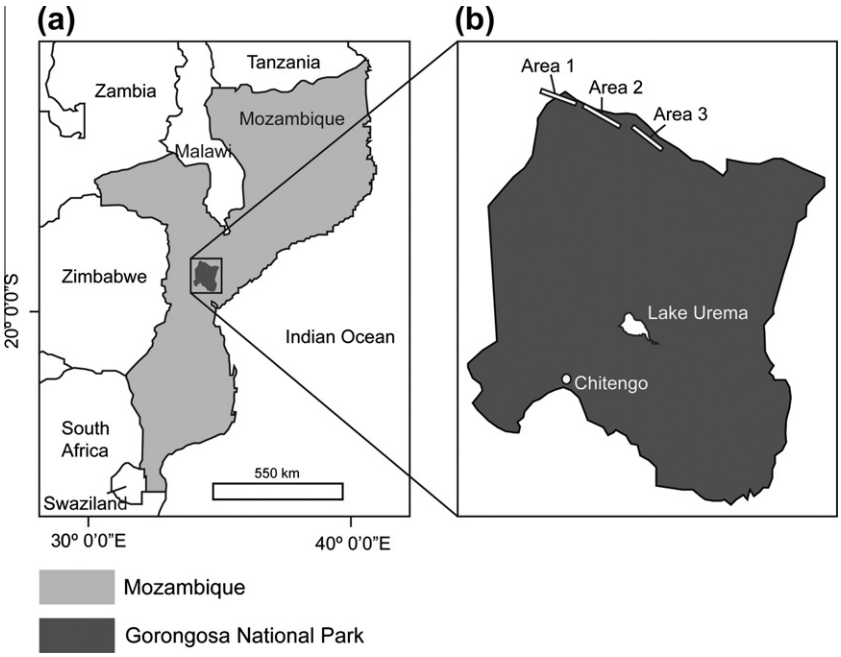

Fig. 1. (a) Map showing the location of Gorongosa National Park in Mozambique, where the study was conducted. (b) Close up on Gorongosa National Park and the location of the three areas in the north of the park.

Lake Urema (LU) in the central part of the park. The lake is a reservoir lake impounded by alluvial fans (Böhme et al., 2006) and due to annual variations in precipitation and evapotranspiration the naturally shallow LU is typified by expansions and withdrawals of its shorelines. The annual amount of precipitation and evapotranspiration varies between the different morphological units and it is only on the Gorongosa Mountain the annual water balance is positive. From here water drains through perennial streams and probably much of the water is recharging groundwater storages along the rift margin. The Nhandugue River is a seasonal sand river which rises from outside the park and crosses the park boundary in the north-western corner (Tinley, 1977). Seasonal means the river has a surface flow that reaches LU only during the rainy seasons. Instead water might be flowing in the sediments from the rift margin and reach LU as groundwater. It was decided to pay special attention to the area where the Nhandugue River flows from the basement gneisses across the western fault margin and onto the rift valley floor sedimentary fill. Field work was conducted in July to August 2009, during the dry season, and data were collected from three areas (Areas 1–3) along the north-western border of GNP (Fig. 1).

1.4. Aim of the research

LU is vital for GNP and park authorities want to predict the effects of changes in different environmental factors in order to maintain sound management and decision-making processes about water resources in the Gorongosa region (Beilfuss et al., 2007). To obtain this information, Gorongosa Research Center in 2007 prepared *Long-term plan for hydrological research: adaptive management of water resources at Gorongosa National Park* (Beilfuss et al., 2007). A result of this plan was a multi-resistivity survey started in 2007, with the aim of obtaining two-dimensional images of the subsurface across the Urema Rift. An initial survey was conducted in 2008 in the downstream area of LU (Chirindja and Hellman, 2009). Evaluation of the results suggested need for further surveys, with additional resistivity profiles. Also it was recommended that reference data is collected in connection to the new resistivity measurements, in order to improve the reliability of the interpretation of the profiles. This study focuses on the western margin of the Urema Rift since it has been anticipated that this area is a potential major groundwater recharge zone to the deeper rift valley floor sediments. The aim is to develop a geological and hydrogeological model for the area in order to understand the infiltration and recharge possibilities for surface water and groundwater.

2. Methods

In order to produce two-dimensional images of the subsurface of the Nhandugue River valley 4-channel multi-electrode gradient array CVES roll-along measurements (Dahlin, 2001) were conducted. An ABEM Lund Imaging System was used, consisting of a Terrameter SAS4000, an Electrode Selector ES10-64C, electrode cables, stainless steel electrodes, etc (ABEM, 2009). An electrode spacing of 5 m was used with a total electrode layout of 400 m, giving a depth penetration around 75 m. Inverse numerical modelling (inversion) was used to produce models of vertical cross sections through the ground, employing Res2dinv (ver.3.58.14) with the robust (L1-norm) inversion constrain (Loke et al., 2003).The computer software Erigraph 2 and EriViz were used for visualizing the models.

In total, resistivity data were collected along nine profiles, three within each of the three study areas (Fig. 3). Due to the high discharge in the rainy seasons and low discharge in the dry seasons the Nhandugue River valley can be divided into three morphological units; (i) a dry-season channel (permanently filled with water), (ii) a wet-season channel (filled with water during rainy seasons) and, (iii) the river flanks. For all three areas a long profile (LP) was placed along the dry-season channel. Each long profile was then crossed by one upstream perpendicular cross profile (CPU) and one downstream perpendicular cross profile (CPD), stretching from the river flanks across the wet-season channel and the dry-season channel.

For geological ground truthing soil samples, from a depth of ~15–30 cm, were collected at locations along the resistivity

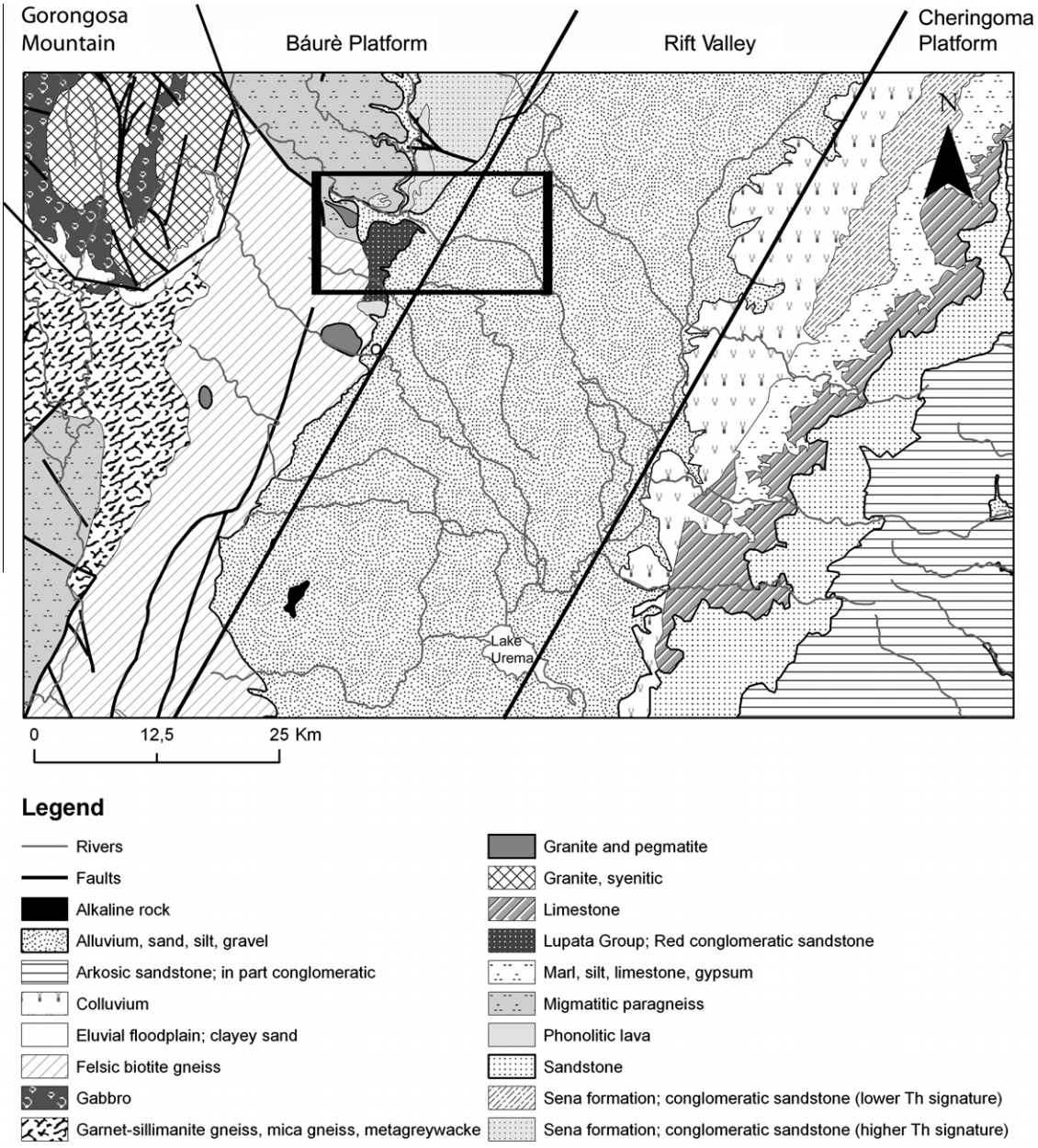

Fig. 2. Geological map of the Urema Rift based on geological data from National Directorate of Geology (2006). The studied area is marked by a black rectangle. Marked are also the four geomorphological units (from left) Gorongosa Mountain, Báruè Platform, Rift Valley and Cheringoma Platform.

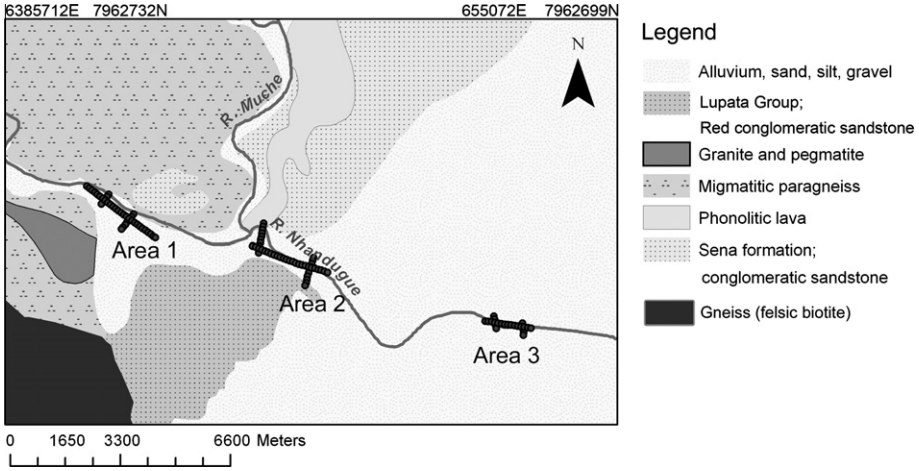

Fig. 3. Location of resistivity profiles in Areas 1–3.

profiles (Fig. 4). In total 21 soil samples were collected for grain size analyses, including sieving and hydrometer analysis. To determine if the soil was permeable enough for water to infiltrate the grain size data were used to calculate the hydraulic conductivity (k). For samples with a uniformity coefficient (C_u) < 5 (after Bowen, 1986) values of k were calculated with Hazen's formula, as defined by Chapuis (2004):

$$k = 1.16 \times d_{10}^2 \quad (1)$$

where d_{10} is Hazen's effective grain size in mm, relative to which 10% of the sample is finer.

To estimate the downstream change in surface discharge (Q) dilution tests were conducted. Tests were conducted on 14th of August 2009 at three locations, one in each area (Fig. 4). In order to get reliable data, sections where the river flowed in one single channel were preferably chosen. For Area 1 this was not possible and measurements were instead conducted in one main channel plus in a smaller channel. The results were then added together. For the tests 500 g of normal table salt (mainly NaCl) was dissolved in 20 L of water and the electrical conductivity (EC) of the solution was measured using an HQ40d Dual-Input Multi-parameter Meter Configurator. By using "EC-masses" ($M \times EC_1$) instead of NaCl-masses it was avoided to have to dry and weigh the salt and to determine the specific relationship between salt and electrical conductivity (Merkel and Steinbruch, 2008). The solution was poured into the stream so that it mixed with the water. At the same time continuous measurements (approximately every second) of the EC was started

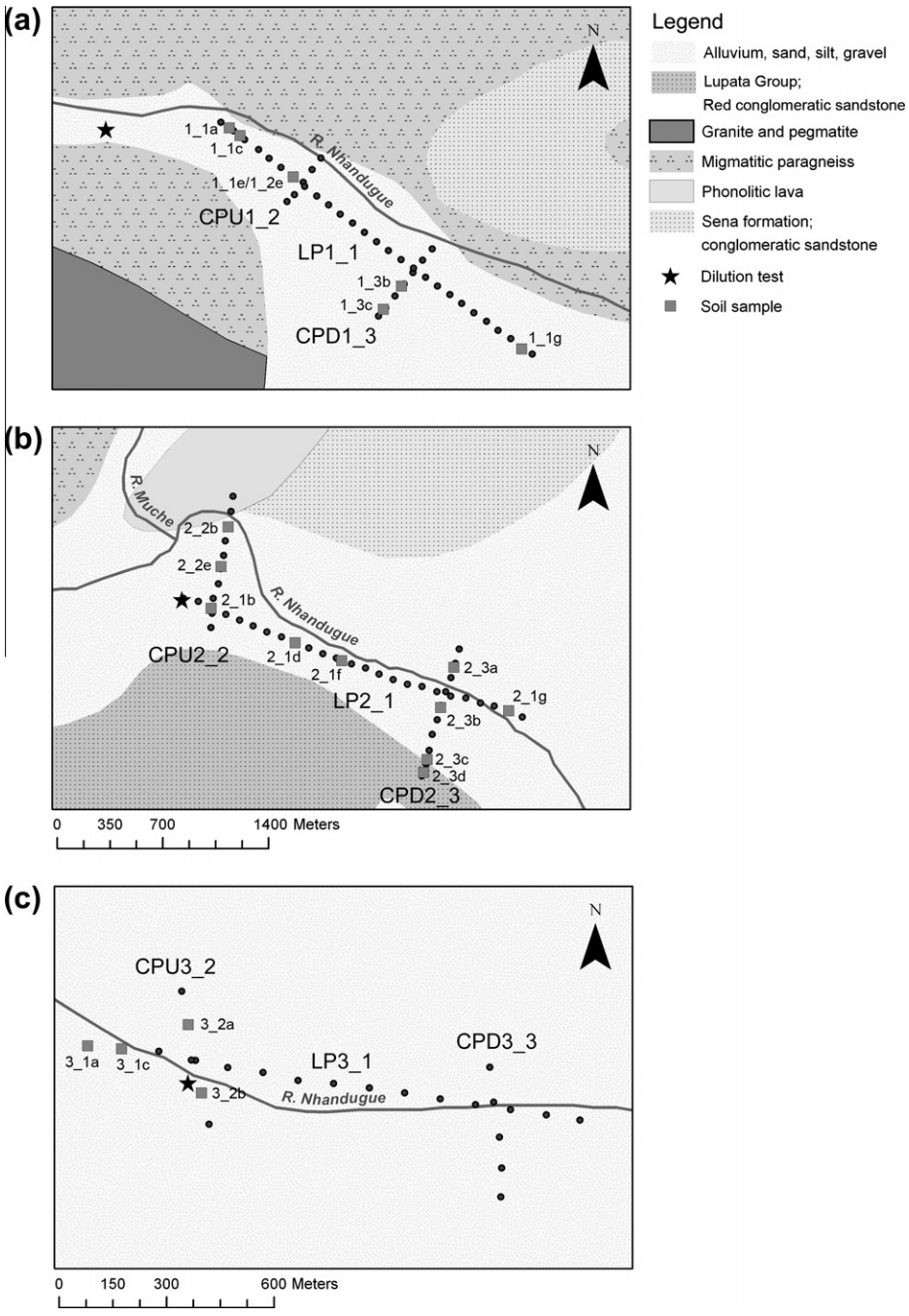

Fig. 4. Close up of Areas 1–3 with locations of soil samples and discharge measurement points marked.

10 m downstream of the injection point. Readings were taken until the conductivity stabilized. Q was then calculated in L/s using Eq. (2), modified from Merkel and Steinbruch (2008):

$$Q = \frac{M \times EC_1}{\int EC} \quad (2)$$

where EC is the electrical conductivity downstream of injection point (μS/cm), M is the amount of water used (L) and EC_1 is the electrical conductivity of the tracer solution (μS).

3. Results

Four main resistivity units are identified for Area 1 (Fig. 5a and b). A top unit with medium to high resistivity (120–1300 Ω m) can be seen in LP1_1. The thickness of the unit varies between 5 m and 15 m. At the edges of CPU1_2, i.e. on the river flanks, this top unit is overlain by two other units, a low resistivity (5–55 Ω m) unit in turn overlain by a medium resistivity (120 Ω m) unit. From the start of LP1_1 and up to 900 m east of the starting point a unit with high resistivity (600–3000 Ω m) is underlying the topmost unit extending to the bottom of the section. Numerous minor vertically oriented heterogeneities can be distinguished in this unit and are marked by vertical lines in Fig. 5a. From 900 m and up to 1500 m another unit, with a medium resistivity (120–600 Ω m), is present. Towards south-east this unit wedges in under a fourth unit of low resistivity (2.2–25 Ω m) that starts at 1300 m. This fourth unit is present in the last ~1300 m of the profile (from 1500 to 2600 m) and has an average thickness of ~60 m.

For Area 2 four resistivity units are identified in the resistivity profiles (Fig. 6a and b). The top unit varies in thickness between ~5 m and 10 m and the resistivity ranges from high to medium (330–1400 Ω m, 37–160 Ω m). The second unit has low resistivity (8.8–37 Ω m) and is discontinuous and varies in thickness between 5 m and 10 m. The third unit is ~15–45 m thick and has a medium resistivity (18–160 Ω m). This unit thickens towards south-east. The bottommost unit stretches all the way to the bottom of the model section, and is thus at least ~15-50 m thick and has low resistivity (2.1–18 Ω m). The unit is found at increasingly larger depths towards south-east. Numerous minor vertical oriented heterogeneities can be distinguished in LP2_1, marked by vertical lines in Fig. 6a.

In the resistivity profiles from Area 3 three resistivity units are clearly identified and a fourth unit is indicated to be present below the third unit (Fig. 7a and b). The top unit is continuously ~5–10 m thick and has medium to high resistivity (37–1400 Ω m). The second unit is somewhat discontinuous with a thickness of ~5–10 m, with a low resistivity (1–18 Ω m). The third unit has a thickness of ~45–50 m and the resistivity is low to medium (18–77 Ω m). The bottom layer is low resistive (<18 Ω m).

From the grain size analyses, the main part of the soil samples from Area 1 are classified as medium and medium to coarse sand (Table 1). One sample (1_1c) is classified as sandy gravel. For Area 2 samples 2_1f and 2_2e are classified as medium sand and samples 2_3b and 2_3d as fine and medium to coarse sand respectively (Table 1). Sample 2_1b and 2_3c are classified as gravelly sand and sandy gravel. Two samples from Area 2 (2_1g and 2_3a) are classified as silty sand and clayey silty sand. Samples 3_1a, 3_1c and 3_2b from Area 3 consist of coarse, medium to coarse and medium sand respectively (Table 1). Two samples from Area 2 (2_1d and 2_2b) and one sample from Area 3 (3_1a) have high organic content (>6%) and grain size analyses could not be performed. The

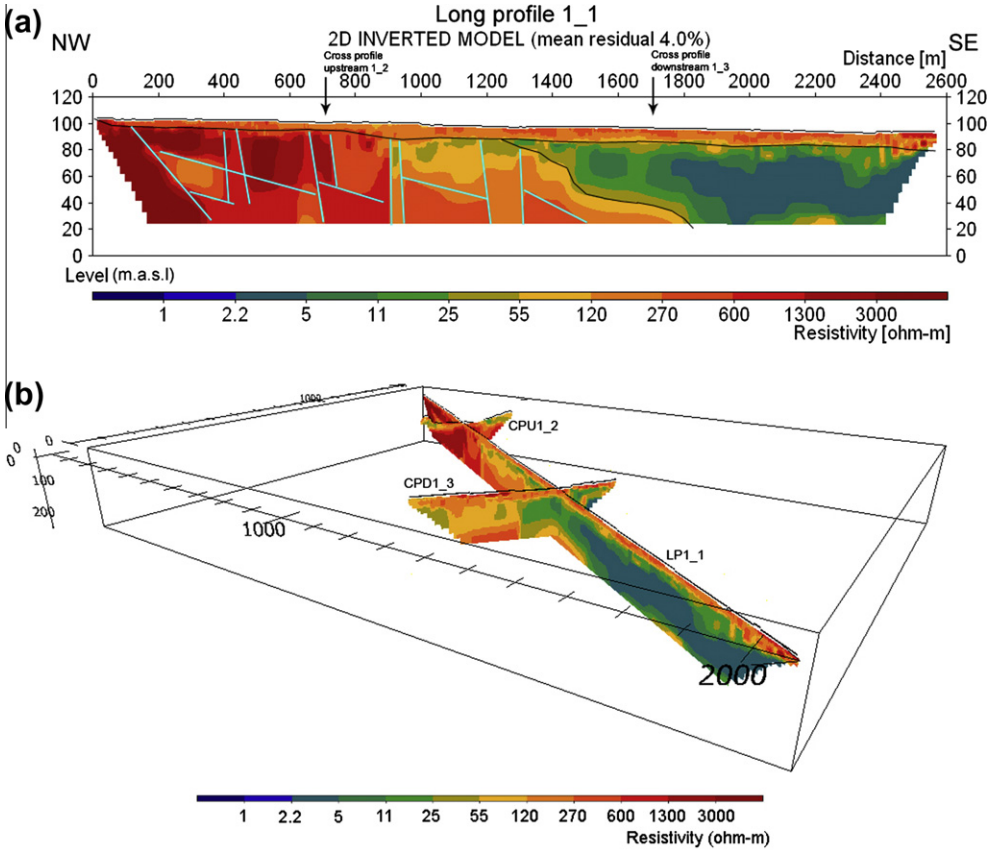

Fig. 5. (a) Resistivity model for profile LP1_1 from Area 1. It shows a thin top unit (orange) and the three units below, 0 to ~900 m (red), ~900 to ~1500 m (orange) and ~1500–2600 m (blue/green), respectively. The blue lines indicate faults. (b) Three-dimensional model of Area 1 showing profiles LP1_1, CPU1_2 and CPU1_3. (For interpretation of the references to color in this figure legend, the reader is referred to the web version of this article.)

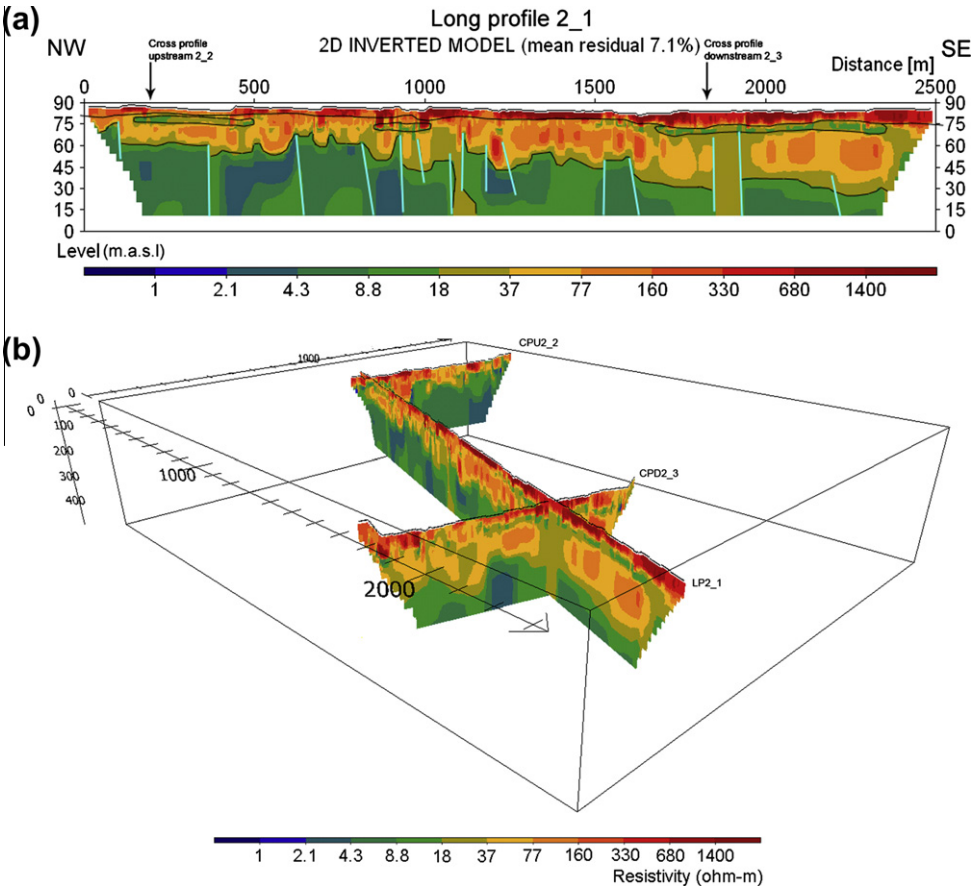

Fig. 6. (a) Resistivity model for profile LP2_1 from Area 2. Four different units can be identified (red, green, orange and blue/green). The blue lines indicate faults. (b) Three-dimensional model of Area 2 showing profiles LP2_1, CPU2_2 and CPU2_3. (For interpretation of the references to color in this figure legend, the reader is referred to the web version of this article.)

hydraulic conductivity in Area 1 ranges from 0.37×10^{-3} to 7.4×10^{-3} m/s. For Area 2 the values range between 0.38×10^{-3} and 2.45×10^{-3} m/s and in Area 3 it ranges from 0.46×10^{-3} m/s to 1.18×10^{-3}.

Just upstream of Area 1, the discharge (Q) was calculated to be 475.74 L/s for the main channel and 88.79 L/s for the small channel. Together they give a total discharge of 564.53 L/s. For measurements just upstream of Area 2 and in Area 3, Q was calculated to 214 L/s and 74 L/s, respectively.

4. Discussion

Fig. 8 is a schematic block model of the interpreted geology. The topmost 10–15 m in all resistivity profiles are highly resistive (Figs. 5–7). This unit is interpreted as alluvial sand, changing from very dry sand at the surface into more moist sand further down. This was visually confirmed during the field work and from the grain size analyses. Below the sand, a highly resistive unit stretches from the start of LP1_1 and up to 900 m (Fig. 5a and b). This unit probably consists of gneiss which is mainly solid, but with fractures indicated by vertical lines in the profiles. The middle section (900–1500 m) in LP1_1 with medium resistivity probably also consist of gneiss, but here it appears to be more fractured and weathered, possibly caused by the presence of water. The vertical and oblique boundary between the sections in LP1_1 probably represents faults in a north-west/south-east direction and in a north/south direction. Vertical heterogeneities are also present in the profiles from Areas 2 and 3, probably indicating fault zones. The faults are most likely minor normal faults that formed simultaneously with the larger faults along the rift margin.

The last section of LP1_1 has low resistivity and most likely consists of saturated sandstone. This is suggested by the presence of outcrops of Sena and Lupata sandstones a few kilometers east of the rift margin. The sandstone in the last section of LP1_1 is most likely also present further downstream, indicated by the bottom-most low resistivity unit in LP2_1 and the low resistivity values in the bottom of LP3_1. Indicated by a dipping of the upper boundary of this unit in the resistivity data the sandstone seems to dip towards east/south-east.

In Areas 2 and 3 a medium resistivity unit is indicated on top of the dipping sandstone. This unit most likely consists of saturated sand mixed with finer material. In LP2_1 and LP3_1 it is indicated that the unit thickens in a downstream direction, which is confirmed by the cross profiles. CPU2_2 shows that the layer is only ~5–10 m thick upstream, while it increases to a thickness of ~40–50 m downstream according to CPU2_3, CPU3_2 and CPU3_3. The sand has most likely been transported from the rift margin and into the rift valley and as the water velocity has decreased the material has been deposited. The thickening of the unit in a downstream direction is probably formed by deposition of material first in lower areas. Between the thickening sand unit and the topmost alluvial sand, low resistive lenses interpreted as lenses of silt and clay are present. In the lower end of the investigated area these lenses appear as a more or less continuous layer.

The calculated values on hydraulic conductivity are 0.37×10^{-3}–7.4×10^{-3} m/s for Area 1, 0.38×10^{-3}–2.45×10^{-3} m/s for Area 2, and 0.46×10^{-3}–1.18×10^{-3} m/s for Area 3.

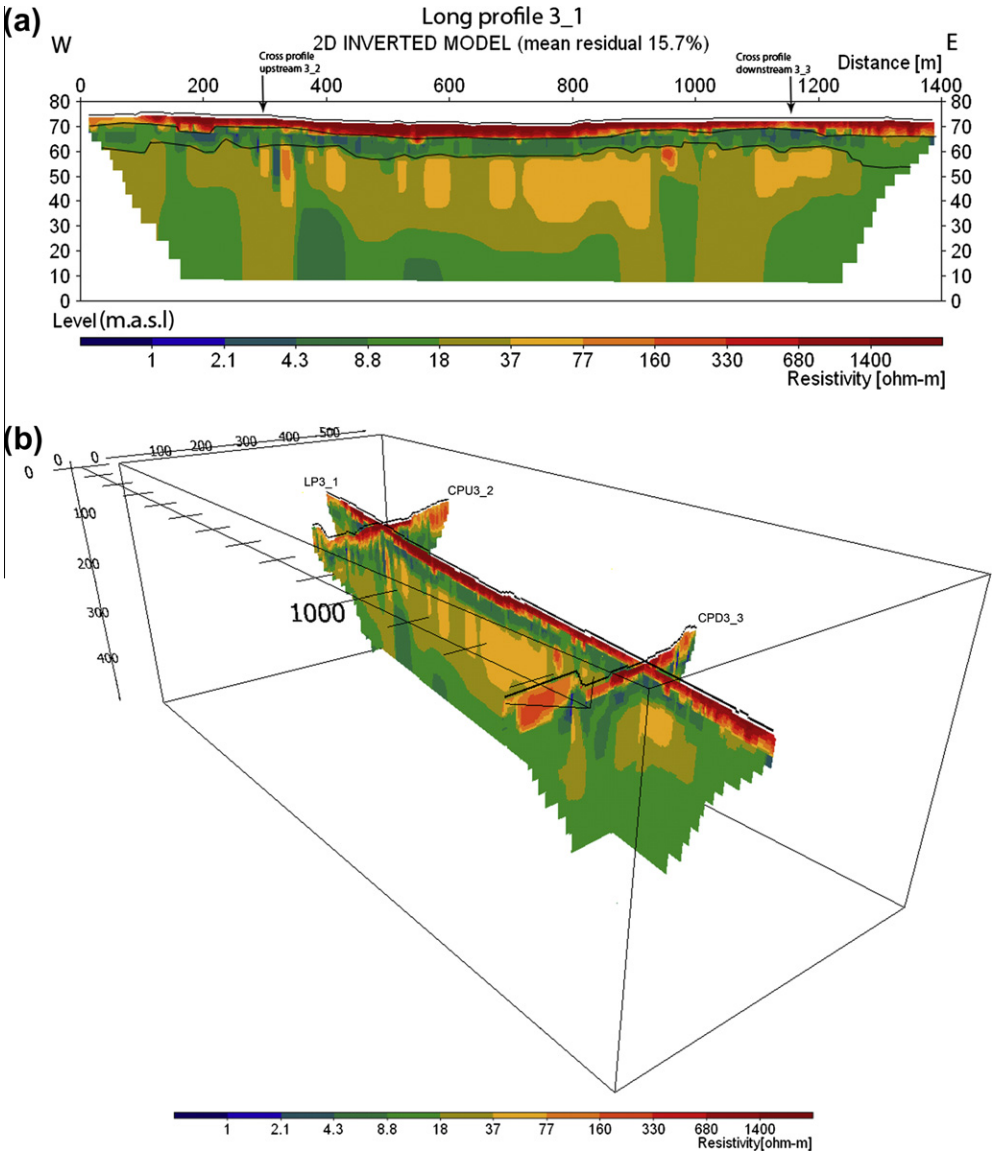

Fig. 7. (a) Resistivity model for the long profile in Area 3. Three different layers can be identified (red, blue/green and orange) and a fourth underlying layer is indicated in the bottom (green). (b) Three-dimensional model of Area 3 showing profiles LP3_1, CPU3_2 and CPU3_3. (For interpretation of the references to color in this figure legend, the reader is referred to the web version of this article.)

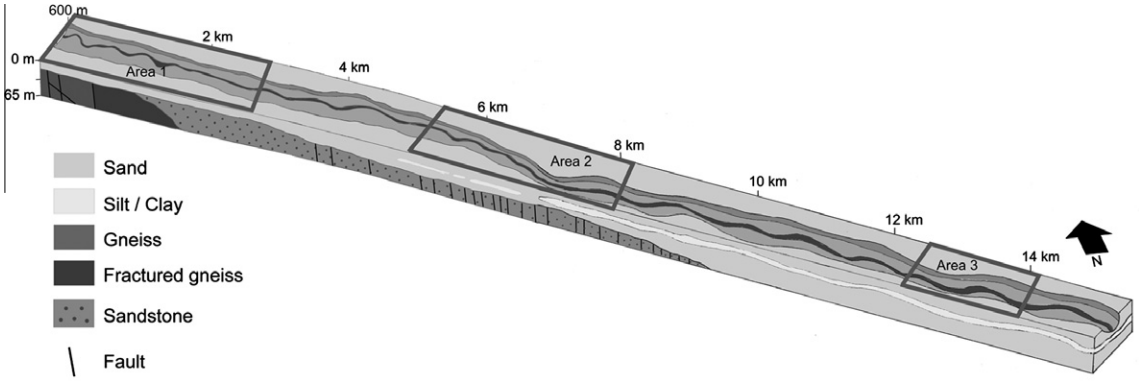

Fig. 8. Schematic block model of the geology in Areas 1–3. Areas 1–3 are marked by black rectangles; Area 1 to the left, Area 2 in the middle and Area 3 to the right. All scales and the extent and location of the different morphological units, i.e. the dry-season channel, wet-season channel and the river flanks, are somewhat approximate. Six different units can be distinguished; (i) a topmost layer of sand, (ii) a unit of solid gneiss, (iii) a unit of fractured gneiss, (iv) a unit of faulted sandstone, (v) a unit of silt and clay and (vi) a unit of sand, mixed with some finer material.

Table 1
Distribution of grain sizes and classification of analyzed soil samples from Areas 1–3.

Sample	Fraction (%)				Classification
	Gravel	Sand	Silt	Clay	
1_1a	0.94	98.91	0.15	0.00	Sand (medium to coarse)
1_1c	52.89	47.11	0.00	0.00	Sandy gravel
1_1e/1_2e	5.51	94.39	0.10	0.00	Sand (medium to coarse)
1_1g	1.48	97.63	0.89	0.00	Sand (medium)
1_3b	1.84	97.47	0.70	0.00	Sand (medium to coarse)
1_3c	6.17	93.19	0.64	0.00	Sand (medium to coarse)
2_1b	28.37	71.24	0.39	0.00	Gravelly sand
2_1f	0.09	99.51	0.40	0.00	Sand (medium)
2_1g	0.19	77.48	13.80	8.53	Silty sand
2_2e	0.00	86.27	6.49	7.24	Sand (fine)
2_3a	0.15	68.84	20.42	10.59	Clayey silty sand
2_3b	1.39	93.35	5.26	0.00	Sand (medium)
2_3c	49.56	47.98	2.47	0.00	Sandy gravel
2_3d	6.23	87.49	6.29	0.00	Sand (medium to coarse)
3_1a	15.31	84.45	0.23	0.00	Sand (coarse)
3_1c	9.17	89.93	0.91	0.00	Sand (medium to coarse)
3_2b	10.72	88.78	0.50	0.00	Sand (medium)

Hence, the values seem to decrease downstream, indicating the material becoming finer further out from the rift margin. The soil samples are on the contrary showing that fine grained material is present in Area 2 but not in Area 3. However, the samples containing fine grained material were less sorted, and as the method used for calculation of hydraulic conductivity states that the uniformity coefficient (C_u) for the sediments has to be <5, values could not be calculated for these samples. Also it is just the maximum values that are decreasing while the lower values are about the same. Hence, the hydraulic conductivity values are somewhat misleading in terms of being related to distance from the rift margin. In this case the location of the samples within the river valley is most likely more important for the sorting of the material and the variation in hydraulic conductivity than the distance from the rift margin. Considering the location of the samples the finer material is located on the river flanks whereas the more sorted materials appear in the closer vicinity of the dry-season channel. This distribution most likely reflects changes in the location of the dry- and wet-season channel and annual variations in discharge.

From the hydraulic conductivity values it is concluded that the topmost alluvial sand is relatively permeable and forms an aquifer. A direct contact between the aquifer and the atmosphere makes it unconfined. Below this aquifer the solid gneiss forms a hydraulic boundary in the west and the fractured gneiss constitutes an unconfined fracture aquifer. Further out from the rift margin the discontinuous layer of finer sediments below the alluvial sand forms an aquiclude through which there is a possibility for leakage in a downward direction. The third unit of alluvial sediments are most likely relatively permeable, hence forming an aquifer. Because of the aquiclude of finer sediments this aquifer is semi-confined. The sandstone unit shows very low resistivities, indicating high porosity and water-saturated conditions. Several small water filled-fracture zones are also most likely present due to heavy faulting. It therefore forms an unconfined aquifer in the west becoming semi-confined down dip where it is overlain by the aquiclude. An east/south-eastward flow direction of the river together with the gentle dip of the sandstone layer is indicating a hydraulic groundwater gradient towards the rift valley floor. This direction is also indicated by the hydraulic boundary in the west and the gently east/south-east sloping ground surface.

The surface discharge for Area 1 has been calculated to ~564 L/s. A true discharge value cannot be given for the main channel in Area 1, due to two major peaks in conductivity instead of one. Still, when comparing the value to the calculated values for Areas 2 and 3 it appears reasonable. In order to get more reliable data it is recommended to repeat and to do continuous measurements, which was not possible in this study due to time limitation. Going about 6 km downstream to the measuring point in Area 2 the water discharge is decreasing to ~214 L/s, and another 7 km downstream, at the measuring point in Area 3, the discharge has decreased to ~74 L/s. Hence, there is a loss in surface water downstream. The river is seasonal and has a wet-season and a dry-season channel. The dry-season channel, in which the discharge measurements were conducted, is meandering within the wider and straighter wet-season channel. Just upstream of Area 1 the river is flowing on bedrock and by the heterogeneity of the surface the dry-season channel is divided into a larger main channel and a couple of smaller channels. Within Area 1 the bedrock becomes overlain by alluvial sediments and the river bed and bank material from there on consists of mainly sandy sediments. The interpreted stratigraphy of the area suggests it is possible for water to infiltrate from the surface to deeper layers. It is therefore suggested that this lost surface water is in parts evapotranspirated and in parts infiltrating downwards, forming groundwater in the lowermost layers.

5. Conclusion

From the resistivity data it can be concluded that east of the rift margin the solid gneiss is fractured and weathered, and overlain by sandstone and Quaternary sediments deposited by alluvial processes. The alluvial sediments are relatively permeable and infiltration of water is possible. The decrease in surface water discharge in the downstream direction is partly attributed to surface water infiltrating into the ground and being transported as groundwater in an east/south-eastward direction, which would confirm that the rift margin is a likely groundwater recharge zone. The east/south-eastward hydraulic gradient further suggests groundwater is flowing towards, and feeds LU.

Acknowledgements

This paper is based on field and laboratory work conducted as part of the M.Sc. theses by K. Arvidsson and L. Stenberg (Arvidsson, 2010; Stenberg, 2010). Research was supervised and enabled by the SIDA-SAREC funded research cooperation between Lund University, Eduardo Mondlane University and GNP. The organization of logistics in the GNP was supported by the Gorongosa Restoration Project and Eduardo Mondlane University in Maputo. USAID funded equipment and staff time in the park. The cost of the field work in Mozambique was supported by two Minor Field Study scholarships from SIDA.

References

ABEM, 2009. Instruction Manual Terrameter SAS 4000/SAS 1000. ABEM Instrument AB, Sundbyberg.

Arvidsson, K., 2010. Geophysical and hydrogeological survey in a part of the Nhandugue river valley, Gorongosa National Park, Mozambique – area 2 and 3. M.Sc. thesis, Department of Earth and Ecosystem Sciences, Lund University, Lund.

Beilfuss, R., Owen, R., Steinbruch, F., 2007. Long-term plan for hydrological research: adaptive management of water resources at Gorongosa National Park. Report Prepared for Gorongosa Research Center, Gorongosa National Park.

Böhme, B., Steinbruch, F., Gloaguen, R., Heilmeier, H., Merkel, B., 2006. Geomorphology, hydrology and ecology of Lake Urema, central Mozambique. J. Phys. Chem. Earth 31, 745–752.

Bowen, R., 1986. Groundwater, second ed. Elsevier Applied Science Publishers, London.

Chapuis, R.P., 2004. Predicting the saturated hydraulic conductivity of sand and gravel using effective diameter and void ratio. Can. Geotech. J. 41, 787–795.

Chirindja, F., Hellman, K., 2009. Geophysical investigation in a part of Gorongosa National Park in Mozamique – a minor field study. M.Sc. thesis, Department of Engineering Geology, Lund University, Lund.

Dahlin, T., 2001. The development of DC resistivity imaging techniques. Comput. Geosci. 27, 1019–1029.
Lächelt, S., 2004. The Geology and Mineral Resources of Mozambique. National Directorate of Geology, Maputo.
Loke, M.H., Acworth, I., Dahlin, T., 2003. A comparison of smooth and blocky inversion methods in 2-D electrical imaging surveys. Explor. Geophys. 34 (3), 182–187.
Merkel, B.J., Steinbruch, F., 2008. Characterization of a Pleistocene thermal spring in Mozambique. Hydrol. J. 16, 1655–1668.
National Directorate of Geology, 2006. Geological Map of Gorongosa, Mozambique. Scale 1:250 000.
Stenberg, L., 2010. Geophysical and hydrogeological survey in a part of the Nhandugue river valley, Gorongosa National Park, Mozambique – area 1 and 2. M.Sc. thesis, Department of Earth and Ecosystem Sciences, Lund University, Lund.
Tinley, K.L., 1977. Framework of the Gorongosa eco system. Ph.D. thesis, Faculty of Science, University of Pretoria, Pretoria.